A Cholesterol Biosensor Based on the NIR Electrogenerated-Chemiluminescence (ECL) of Water-Soluble CdSeTe/ZnS Quantum Dots

Alasdair J. Stewart,[a,b] Emmet J. O'Reilly,[b,c] Roisin D. Moriarty,[b] Paolo Bertoncello,[d] Tia E. Keyes,[b] Robert J. Forster[b] and Lynn Dennany[a]*

[a]*WestCHEM. Department of Pure and Applied Chemistry, University of Strathclyde. 295 Cathedral Street, Glasgow, G1 1XL*

[b]*National Biophotonics& Imaging Platform Ireland, School of Chemical Sciences, Dublin City University, Dublin 9, Ireland*

[c]*Department of Chemical and Environmental Science, Materials and Surface Science Institute, University of Limerick, Limerick, Ireland.*

[d]*College of Engineering, Multidiscplinary Nanotechnology Centre and Centre for NanoHealth, Swansea University, Swansea, SA2 8PP, UK.*

[*] To whom correspondence should be addressed.

ABSTRACT

This contribution examines the application of near infra-red (NIR) quantum dot (QD) containing films for cholesterol detection. Water-soluble, 2-(dimethylamino)ethanthiol (DAET) protected 800 nm CdSeTe/ZnS core-shell QDs were prepared and incorporated into a chitosan film. The NIR electrogenerated chemiluminescence (ECL) of the QD/chitosan films upon reaction with H_2O_2 co-reactant (produced as a by-product of cholesterol oxidase-catalysed oxidation of cholesterol) gave a strong ECL signal at -1.35 V vs. Ag/AgCl. The sensor displayed a linear response over the clinically relevant range ($0.25 \leq$ [cholesterol] ≤ 5 mM) allowing the rapid detection of cholesterol and providing a platform for future development. Significantly, this NIR emission has been shown to exhibit excellent penetrability through biological samples, and will likely be at the forefront of development in the biosensing and imaging fields for the foreseeable future.

INTRODUCTION

The burden of high cholesterol levels on healthcare services worldwide is becoming an increasing problem as over-eating and lack of exercise drive the current global obesity epidemic. Hypercholesterolemia (total blood cholesterol concentrations above 5mM),[1]caused by a diet high in saturated fat[2] results in the accumulation of cholesterol on arterial walls, leading to hardening, thinning and chronic inflammation (atherosclerosis)[3]Patients suffering from this indisposition are at a proven risk of developing more serious cardiac related diseases such as ischaemic heart disease[4-5], stroke[6] and peripheral vascular disease.[7] Detection of elevated cholesterol levels is therefore key in implementing a strategic health plan to reduce total cholesterol blood concentrations and minimize the risk of progression to more serious diseases.[8]Literature in this area indicates that it is the levels of high density and low density lipoproteins that are most strongly indicative of cardiovascular disease risk.[8-10] Both low levels of high density lipoproteins (HDL) and high levels of low density lipoproteins (LDL) are associated with an increased risk of CVD.[11] This is because oxidation of LDL tends to promote the development of atherosclerosis,[12] whereas HDL has a host of benefits that fight its onset.[13] Levels of these lipoproteins can be estimated via their associated cholesterol concentrations.[14] As such the requirement for accurate, robust and selective biosensors for cholesterol detection is of clear clinical importance.

A number of cholesterol detection methods based on spectrophotometric[15], HPLC[16] and gas-liquid chromatography[17] have previously been reported. However, these tend to require expensive equipment, extensive sample preparation and suffer from poorer sensitivity and selectivity when compared to enzymatic based techniques. As such the majority of cholesterol biosensors incorporate cholesterol oxidase (ChOx) into their design and use electrochemical detection (amperometric) of hydrogen peroxide, produced as a byproduct in the ChOx-catalysed oxidation of cholesterol in the presence of oxygen.[18-22] The presence of ChOx infers excellent

inherent selectivity, avoiding the need for lengthy sample preparation procedures and reducing costs, however, interference from other analytes present in the sample, as with any analysis, can lead to errors in interpretation.

ECL has been used extensively as a detection method in bio-sensing because of its advantages over other detection techniques. Excellent sensitivity is achieved as no light source is required, resulting in minimal background light intensity[23], whilst scattered light and interferences from emission by impurities or other analytes is effectively eliminated.[24] Combined with the specificity of the ECL reaction, these attributes produce a technique that is ideally suited for detecting low concentration target analytes in complex matrices with a good signal to noise ratio.[25-28] These benefits have allowed the development of a variety of ECL-based biosensors for cholesterol detection. Marquette *et al*[29] developed a biosensor based on the ECL of a luminol/H_2O_2 system, with ChOx immobilised in a membrane through which the cholesterol samples were passed. Generation of H_2O_2 in the presence of cholesterol resulted in the emission of ECL from luminol, allowing detection down to 0.6nM. Ballesta-Claver*et al*[30] created a disposable sensor that incorporated synthesized luminol copolymers onto which ChOx was covalently attached. In the presence of cholesterol, production of H_2O_2 resulted in the generation of ECL from these conducting polymers that showed a linear response to increasing cholesterol concentrations.

Clearly, one of the most important aspects of enzymatic-based sensors is that the bioactivity, stability and specificity of the enzymatic reaction is retained in both the conditions and/or immobilization techniques used. A number of immobilization matrices have been reported previously, including sol-gel films[31-33], polyaniline films[34-35], polypyyrole films[36-38] and a selection of other conducting polymer films.[39-41] However, more recently, the use of nano-

materials as immobilization matrices have been pursued. Their large surface area relative to bulk size provides a high enzyme loading ability and a compatible microenvironment allows retention of bioactivity. QDs in particular, have found uses in a broad range of bio-sensing applications because of their unique optical and electronic properties and have been widely used in ECL systems following their discovery as ECL emitters by Bards group in 2002.[42] Their high quantum efficiency and resistance to photo-bleaching, combined with their size-tuneable emission, make them ideal luminophores, whilst their large surface area allows greater biomolecule loading than standard emitters. Zhu *et al*[43] developed a cholesterol biosensor with ChOx immobilised on gold nanoparticle-decorated multiwalled carbon nanotubes. The use of nanoparticles allowed high enzyme loading and fast electron transfer rates with amperometric detection being used to determine cholesterol concentrations. Hong *et al*[44] used cupric oxide nanoparticles to catalyse the oxidation of luminol by H_2O_2. The sensitivity of this chemiluminescent sensor was improved when compared to the same system with no nanoparticles present.

However, at the time of writing there does not appear to be any work based on the ECL of near-infrared (NIR) QD films for the detection of cholesterol. The benefit of such a system is that emission above 800 nm reduces signal interference from whole blood samples, an issue that can affect detection systems that use emitters in the visible region. These NIR emitters can therefore act as a gateway for development of a cholesterol sensor that can directly analyze whole blood samples with no sample pre-treatment.

In this work, we have developed a biosensor for cholesterol based on the ECL of 800 nm CdSeTe/ZnS core-shell QDs (Figure 1). A glassy carbon electrode (GCE) was modified with a QD/chitosan composite. Chitosan was selected as the polymer for film development due to its

non-toxicity, good biocompatibility and commercial availability.[45-46] This work has shown that these water-soluble, NIR-emitting QDs are suitable for use in ECL biosensors and could be extremely helpful in the development of novel systems that are able to detect clinically relevant analytes directly from clinical samples. They have been used to successfully develop a cholesterol detection system with a clinically-relevant linear range, minimizing the requirement for sample preparation. Ideally, this system could be used in combination with an agent that has the ability to selectively release cholesterol from HDL and LDL prior to its quantification and is an area in which future work would focus.

EXPERIMENTAL SECTION

Materials and Methods

Core-shell CdSeTe/ZnSquantum dots (Qdot® 800 ITK™ organic quantum dots, 1μM in decane) were purchased from Invitrogen. Chitosan (medium molecular weight, 75-85% deacetylated), phosphate buffered saline (PBS, pH 7.4), hydrogen peroxide, cholesterol, cholesterol oxidase (ChOx) from *Streptomyces sp.*, 2-(dimethylamino)ethanthiol (DAET) and 25% aqueous glutaraldehyde were all purchased from Sigma-Aldrich and used as received. All other chemicals were of reagent grade quality and used as received. Human serum samples were obtained from Dublin City University following ethical approval and stored at -20°C until use.

Glassy carbon electrodes (3mm diameter)were purchased from IJ Cambria (UK). They were cleaned by successive polishing using 1, 0.3 and 0.05 μm alumina slurry, followed by sonication in ethanol and water, respectively, for 30 minutes. Measurements involving simultaneous detection of light and current utilized a CH instrument model 760D connected to a Hamamatsu H6780-20 PMT powered at -950 V.

During the ECL experiments, 1 mL sample volume was required and run time was 40 s. The cell was kept in a light-tight Faraday cage in a specially designed holder configuration where the working electrode was positioned directly above the PMT window. All electrochemical experiments were carried out using a conventional three-electrode assembly. Potentials are quoted *versus* Ag/AgCl using a platinum wire as counter and all measurements were made at room temperature (20°C). All other reagents used were of analytical grade, and all solutions were prepared in Milli-Q water (18 mΩ cm). ECL spectra were recorded on Ocean Optics USB2000+ CCD spectrometer using CH instriument electrochemical analyser, CH instrument model 760D.

Preparation of water soluble CdSeTe/ZnS core-shell QDs

The method followed was similar to that developed by Woelfle and Claus[47]. 0.5 mL of 0.5 M DAET in methanol was mixed with 0.25 mL of the CdSeTe/ZnS QDs in decane (1μM). Nitrogen was bubbled through the solution for 5 minutes, which was then sealed and left stirring overnight at room temperature in the dark. The QDs were then precipitated with an excess of acetone followed by centrifugation at 5000 rpm for 6 minutes. The filtrate was removed and the precipitate was re-dispersed in 0.25 mL of distilled water. These water-soluble QDs were centrifuged for a further 6 minutes at 3000 rpm to remove any impurities and then stored in darkness in the fridge.

Preparation of CdSeTe/ZnS core-shell QD-chitosan composite film

0.1% chitosan was prepared by dissolving 1.1 mg chitosan in 1 mL of 1% aqueous acetic acid. The QD/chitosan composite was prepared by mixing aliquots of the water-soluble QDs with the chitosan solution in a 1:1 (v/v) ratio. This composite was then carefully cast onto the electroactive portion of a GCE and allowed to dry in the fridge for 1 hour in the dark.

Cholesterol and cholesterol oxidase solution preparation

5 mL of Triton X-100 and 5 mL of isopropanol were mixed and heated to 50°C. 0.1933 g of cholesterol was slowly added to this solution until fully dissolved and then 40 mL of 0.1 M PBS was added with continuous mixing to produce a 10 mM stock solution. A cloudy solution resulted, which became clear after cooling. The solution was stored in the fridge (4°C) when not in use and required gentle heating, to 35°C, and cooling if it turned cloudy. Aliquots of this stock

solution were diluted in Triton X-100:isopropanol:0.1 M PBS (1:1:8) to obtain the required cholesterol concentrations for analysis.

A 10 mg/mL ChOx stock solution was prepared on the day of use by dissolving 1 mg of ChOx in 100 µL of distilled water.A 1 in 10 dilution of this ChOx solution was made in cholesterol solutions at varying concentrations, giving a working concentration of 0.1 mg/mL. The modified electrode was immersed in these solutions, which had been incubated for 60 minutes at 45°C to allow oxidation of cholesterol to occur. The incubation temperature was set at 45°C as maximum activity of Cholesterol Oxidase from *Streptomyces sp.* is achieved at this temperature (according to manufacturer). A scanning potential between 0 and -2 V was then applied to the modified electrodes and the ECL signal was monitored using a photomultiplier tube (PMT).

Preparation of spiked interferent samples

A 5 mM cholesterol solution was prepared in Triton X-100:isopropanol:0.1 M PBS (1:1:8) to which 10 mM urea, 10 mM glucose or 1 mg/mL citric acid was added. This solution was then incubated with ChOx as outlined above and the ECL response of the QD/chitosan film was then monitored.

Preparation of spiked and unknown human serum samples

Human serum was mixed 1 to 1 with cholesterol solutions at different concentrations containing 0.1 mg/mL ChOx. These solutions were mixed and left to incubate for 60 minutes at 45°C and then analyzed by ECL.

Preparation of CdSeTe/ZnS core-shell QD-chitosan-ChOx composite film

Water-soluble CdSeTe/ZnS QDs were dropcast onto the electrode and left to dry in the fridge for 1 hour. 0.05% chitosan was then dropcast on top of this film and allowed to dry in the fridge for 1 hour. This film was then incubated in 10% glutaraldehyde for 1 hour at room temperature followed by washing with distilled water. The electrode was then incubated in a 10 mg/mL solution of ChOx for 3 hours at room temperature followed by washing in PBS-Tween and distilled water. These films were then immersed in solutions of cholesterol and immediately analyzed.

RESULTS AND DISCUSSION

Characterisation of the QD/chitosan composite film. The absorption and emission profiles of the QDs are shown in Table 1. Examination of the QDs was undertaken utilizing emission spectrometry. The emission maximum for the QDs lies at ~795 nm. This is related to the radiative recombination of electrons, which have been excited into higher energy levels of the QD following photon absorption, as they return to the ground state.

The ECL spectrum of the QDs, Fig. 2, shows an emission peak at approximately 810 nm, ~15 nm longer than the photo-induced emission peaks of the QDs. This red shifted wavelength associated with the surface-confined electrochemical reactions leading to emission in the ECL process is most likely due to the difference in the reorganization energy of this route when compared to standard, optically-induced emission, as seen previously.[26-27, 48-50]

The electrochemical characteristics of a blank GCE and the QD/chitosan films in the presence and absence of H_2O_2 and in the presence of cholesterol were investigated using cyclic voltammetry (CV) and are shown in Fig. 3. When no QD/chitosan film is present, no discernable peaks are observed. Following QD/chitosan film application, a peak is observed at -1.8 V *vs.* Ag/AgCl in all cases. Investigations into this peak (see supplementary data) suggested it was related to a secondary reduction of the QDs themselves, which resulted in their destruction. When H_2O_2 is introduced into the system, either directly or via cholesterol oxidation, two additional irreversible reduction processes are observed at approximately -1.35 V and -1.55 V *vs.* Ag/AgCl. The peak at -1.35 V is related to the concentration of H_2O_2 (peak current increases with increasing H_2O_2 concentration – see supplementary data), suggesting it is associated with its direct reduction or the reduction of one of its degradation products, such as the formation of hydroxyl ions from hydroxyl radicals. The peak at -1.55 V is likely related to a similar process,

but may involve reduction of a species created following electron transfer between film components, causing this increase in peak potential.

In the presence of an incubated cholesterol/ChOx solution, the same reduction peaks are observed as when H_2O_2 is present, indicating that oxidation of cholesterol has been successful and H_2O_2 has been produced following reduction of dissolved oxygen. H_2O_2 can then act as a co-reactant for the production of ECL from the QDs through the following electrochemical reactions:[51-52]

$$QDs + 1e^- \rightarrow QDs(e^-1_{Se}) \quad (1)$$

$$QDs(e^-1_{Se}) + H_2O_2 \rightarrow QDs + OH^- + OH^\bullet \quad (2)$$

$$OH^\bullet + QDs \rightarrow OH^- + QDs(h^+1_{Sh}) \quad (3)$$

$$QDs(e^-1_{Se}) + OH^\bullet \rightarrow OH^- + QDs^* \quad (4)$$

$$QDs(e^-1_{Se}) + QDs(h^+1_{Sh}) \rightarrow QDs^* \quad (5)$$

$$QDs^* \rightarrow QDs + h\nu\ (800\ nm) \quad (6)$$

Initially, electrons are injected into the 1Se quantum confined orbital of the QDs to create electron-injected QD intermediates (equation (1)) that are capable of reducing H_2O_2 to OH^- and $OH^\bullet$ (equation (2)) following a simulated Haber-Weiss reaction. Typically, this requires superoxide, O_2^-, generated through the single electron reduction of oxygen. However, in this case, $QDs(e^-1_{Se})$ acts as the radical anion in place of superoxide to reduce H_2O_2 to $OH^\bullet$. This hydroxyl radical is the crucial species for ECL production in this system and following its formation is reduced in the process of injecting a hole into the 1Sh quantum confined orbital of a QD to create hole-injected QDs, $QDs(h^+1_{Sh})$ (equation (3)). This process is favorabledueto the

high standard redox potential of the $OH^-/OH^\bullet$ couple. Excited state QDs (QDs*) can then be formed via an annihilation or co-reactant pathway. Hole-injected QDs can recombine with electron-injected QDs to create QDs* via the annihilation route (equation (5)), whilst reduced QDs can also interact directly with $OH^\bullet$ to create QDs* following the co-reactant route (equation (4)). Both of these processes result in the formation of QDs*, which will relax to the ground state accompanied by the emission of light at a wavelength determined by the band gap, and therefore size, of the QD material. In the presence of H_2O_2, two ECL peaks were present, which has been observed previously.[46] The initial peak, ECL-1, was shown to result from the interaction of a nanocrystal species formed due the reduction of the QDs and the co-reactants, whilst ECL-2 is produced from the interaction of the co-reactants and the assembly of QD reduced nanocrystal species. Investigations in this study, showed that ECL-2 is more sensitive to the dissolved H_2O_2, and thus was chosen to detect H_2O_2 for developing ECL sensing applications of these QD/chitosan films.

ECL of the QD/chitosan composite film. Fig. 4 illustrates the ECL response of the QD/chitosan composite film as a function of H_2O_2concentration. An ECL peak is seen at approximately -1.35 V *vs.* Ag/AgCl, with intensity increasing linearly with increasing H_2O_2 concentrations from 0.25 to 2 mM. This peak is closely related to the reduction process seen in the CVs at a very similar potential, indicating the two events are closely related and that ECL emission is dependent upon this process.[46]

Reproducibility was improved by using small volumes, below 1.5 μL of QD/chitosan which reduced the possibility of aggregation of the QDs in the film which might lead to variations in the ECL response.

Quantitative Detection of Cholesterol. In the presence of ChOx, H_2O_2 is produced as a by-product of cholesterol oxidation and can then act as a co-reactant for the production of QD ECL, in the reactions described previously (equations 1 – 6). As a linear ECL response to H_2O_2 has been achieved, it is proposed that QD/chitosan film ECL could be used for the quantitative detection of cholesterol. Fig. 5 shows the ECL response of the QD/chitosan films to increasing cholesterol concentrations.

The ECL signal shows a linear dependence over the range 0.25-5 mM cholesterol. The ECL spectrum is consistent with those acquired using H_2O_2 co-reactant, as shown in Fig. 4. This indicates that H_2O_2 is successfully being produced at a concentration dependent upon the cholesterol concentration and can therefore be utilized to monitor cholesterol concentration. As such, an increase in ECL intensity is seen with an increase in total cholesterol concentration. Above 5 mM, the ECL response deviates from linearity; however this is above the medical cut-off for high cholesterol.[8] The response from multiple biosensors was investigated to determine the reproducibility of this system and is shown in Fig. 6.

This shows a reproducible linear response to increasing cholesterol concentrations from three independent biosensors, highlighting the consistent behaviour of this system. QD stability over a three week period was examined to give an indication of the shelf-life of this biosensor (supplementary information, Fig. S2). A consistent ECL response from the QDs is apparent over the considered period, with a drop in intensity of only 5.2% after three weeks. Response variability increases at the three week point, indicating biosensor reproducibility may suffer after this time.

In order to determine the clinical viability and cross-reactivity of this system, the influence of interferents commonly found in clinical samples (glucose, urea, citric acid) on the ECL response of this biosensor in 5 mM cholesterol is shown in Fig. 7.

None of these had any appreciable effect on the observed ECL intensity indicating good sensor specificity. Therefore, human serum samples were spiked with increasing cholesterol concentrations and the response of the QD/chitosan film in each sample was measured (Fig. 8). A linear range from 1.5 to 4.5 mM cholesterol was examined and the ECL responses were used to quantify cholesterol in spiked serum samples. Table 2 described the results obtained for the spiked serum samples, showing an averaged recovery of 93% over the concentrations examined.

These results show that this specific system can be used to determine cholesterol concentrations from human serum samples, confirming the viability of this biosensor. In order to progress the development of this sensor, the incubation step was removed and evaluation of the QD film ECL response following immobilization of ChOx on the electrode surface was investigated. Figure 9 shows the response of these QD/chitosan/ChOx films to increasing cholesterol concentrations.

As with ChOx in solution, a peak at approximately -1.35 V *vs.* Ag/AgCl was observed, with the ECL intensity linearly dependent upon the cholesterol concentration. The linear range was expanded to examine the concentration range 0 mM ≤ [cholesterol] ≤7 mM cholesterol. This suggests that the system is sufficiently sensitive to detect H_2O_2 even without an incubation step, opening up possibilities for future development into a more rapid, convenient biosensor for cholesterol detection.

CONCLUSIONS

An ECL biosensor for the determination of total blood cholesterol was demonstrated using water-soluble CdSeTe/ZnS core-shell QDs. Electrodes modified with thin films containing these NIR ECL QDs were used to monitor the cholesterol concentrations as a result of the production of H_2O_2 during the ChOx-catalyzed oxidation of cholesterol. The ECL response showed good linear dependence on cholesterol concentrations over the clinically relevant range. This system was then successfully used to generate a linear calibration plot for cholesterol in spiked human serum samples and to quantify cholesterol in unknown human serum samples. As far as the authors know, this is one of the first ECL biosensors based on NIR emission from QD films examining the applicability of these sensors for blood serum analysis. The major advantage of this is the much improved penetrability of the ECL signal through biological samples, paving the way for developments in whole blood point-of-care biosensing based on these nano-architectured surfaces. Future studies will examine interferences, storage stability as well as pH and temperature effects for the integration of this biosensor in a lab-on-a-chip system.

REFERENCES

1. Durrington, P., *The Lancet* **2003,** 362, (9385), 717-731.

2. Tan, M.; Dickinson, M.; Albers, J.; Havel, R.; Cheung, M.; Vigne, J., *The American journal of clinical nutrition* **1980,** 33, (12), 2559-2565.

3. Kovala, J. P., *Cholesterol in Atherosclerosis and Coronary Heart Disease*. Nova Science Pub Incorporated: 2005.

4. Castelli, W. P.; Anderson, K., *The American Journal of Medicine* **1986,** 80, (2, Supplement 1), 23-32.

5. Ezzati, M.; Lopez, A. D.; Rodgers, A.; Vander Hoorn, S.; Murray, C. J. L., *The Lancet* **2002,** 360, (9343), 1347-1360.

6. Collins, R.; Armitage, J.; Parish, S.; Sleight, P.; Peto, R.; null, *Lancet* **2004,** 363, (9411), 757-767.

7. Aspry, K. E.; Holcroft, J. W.; Amsterdam, E. A., *American journal of preventive medicine* **1995,** 11, (5), 336-341.

8. Gordon, D. J.; Probstfield, J. L.; Garrison, R. J.; Neaton, J. D.; Castelli, W. P.; Knoke, J. D.; Jacobs, D. R.; Bangdiwala, S.; Tyroler, H. A., *Circulation* **1989,** 79, (1), 8-15.

9. Castelli, W. P.; Garrison, R. J.; Wilson, P. F.; Abbott, R. D.; Kalousdian, S.; Kannel, W. B., *JAMA* **1986,** 256, (20), 2835-2838.

10. Bonow, R. O., *Circulation* **2002,** 106, (25), 3140-3141.

11. Mathieu, P.; Pibarot, P.; Larose, É.; Poirier, P.; Marette, A.; Després, J.-P., *The international journal of biochemistry & cell biology* **2008,** 40, (5), 821-836.

12. Stocker, R.; Keaney, J. F., *Physiological reviews* **2004,** 84, (4), 1381-1478.

13. Navab, M.; Reddy, S. T.; Van Lenten, B. J.; Fogelman, A. M., *Nature Reviews Cardiology* **2011,** 8, (4), 222-232.

14. Cui, Y.; Blumenthal, R. S.; Flaws, J. A.; Whiteman, M. K.; Langenberg, P.; Bachorik, P. S.; Bush, T. L., *Archives of Internal Medicine* **2001,** 161, (11), 1413-1419.

15. Kenny, A., *Biochemical Journal* **1952,** 52, (4), 611.

16. Wong, W. W.; Hachey, D. L.; Clarke, L. L.; Zhang, S.; Llaurador, M.; Pond, W. G., *Applied radiation and isotopes* **1994,** 45, (4), 529-533.

17. Agulló, E.; Gelós, B. S., *Food research international* **1996,** 29, (1), 77-80.

18. Tan, X.; Li, M.; Cai, P.; Luo, L.; Zou, X., *Anal Biochem* **2005,** 337, (1), 111-120.

19. Vidal, J.-C.; Espuelas, J.; Garcia-Ruiz, E.; Castillo, J.-R., *Talanta* **2004,** 64, (3), 655-664.

20. Crumbliss, A.; Stonehuerner, J.; Henkens, R.; Zhao, J.; O'Daly, J., *Biosensors and Bioelectronics* **1993,** 8, (6), 331-337.

21. Guo, M.; Chen, J.; Li, J.; Nie, L.; Yao, S., *Electroanalysis* **2004,** 16, (23), 1992-1998.

22. Brahim, S.; Narinesingh, D.; Guiseppi-Elie, A., *Analytica chimica acta* **2001,** 448, (1), 27-36.

23. Arora, A.; Eijkel, J. C. T.; Morf, W. E.; Manz, A., *Analytical Chemistry* **2001,** 73, (14), 3282-3288.

24. Fan, F.-R. F., *Electrogenerated Chemiluminescence*. 1 ed.; Marcel Dekker, Inc.: New York, 2004; Vol. 1, p 540.

25. Qi, H.; Peng, Y.; Gao, Q.; Zhang, C., *Sensors* **2009,** 9, (1), 674-695.

26. Venkatanarayanan, A.; Spehar-Délèze, A.-M.; Dennany, L.; Pellegrin, Y.; Keyes, T. E.; Forster, R. J., *Langmuir* **2008,** 24, (19), 11233-11238.

27. O'Reilly, E. J.; Keyes, T. E.; Forster, R. J.; Dennany, L., *Analyst* **2013,** 138, (2), 677-682.

28. Devadoss, A.; Dennany, L.; Dickinson, C.; Keyes, T. E.; Forster, R. J., *Electrochemistry Communications* **2012,** 19, (0), 43-45.

29. Marquette, C. A.; Ravaud, S.; Blum, L. J.,*Analytical Letters***2000**, 33, (9), 1779-1796.

30. Ballesta-Claver, J.; Ametis-Cabello, J.; Morales-Sanfrutos, J.; Megía-Fernández, A.; Valencia-Mirón, M.; Santoyo-González, F.; Capitán-Vallvey, L., *Analytica chimica acta* **2012**, 754, 91-98.

31. Kumar, A.; Malhotra, R.; Malhotra, B.; Grover, S., *Analytica chimica acta* **2000,** 414, (1), 43-50.

32. Li, J.; Peng, T.; Peng, Y., *Electroanalysis* **2003,** 15, (12), 1031-1037.

33. Singh, S.; Singhal, R.; Malhotra, B., *Analytica chimica acta* **2007,** 582, (2), 335-343.

34. Wang, H.; Mu, S., *Sensors and Actuators B: Chemical* **1999,** 56, (1), 22-30.

35. Singh, S.; Solanki, P. R.; Pandey, M.; Malhotra, B., *Sensors and Actuators B: Chemical* **2006,** 115, (1), 534-541.

36. Vidal, J. C.; García, E.; Castillo, J. R., *Analytica chimica acta* **1999,** 385, (1), 213-222.

37. Singh, S.; Chaubey, A.; Malhotra, B., *Analytica chimica acta* **2004,** 502, (2), 229-234.

38. Singh, S.; Chaubey, A.; Malhotra, B., *Journal of applied polymer science* **2004,** 91, (6), 3769-3773.

39. Akkaya, B.; Şahin, F.; Demirel, G.; Tümtürk, H., *Biochemical Engineering Journal* **2009,** 43, (3), 333-337.

40. Dennany, L.; Forster, R. J.; Rusling, J. F., *Journal of the American Chemical Society* **2003,** 125, (17), 5213-5218.

41. Dennany, L.; Forster, R. J.; White, B.; Smyth, M.; Rusling, J. F., *Journal of the American Chemical Society* **2004,** 126, (28), 8835-8841.

42. Ding, Z.; Quinn, B. M.; Haram, S. K.; Pell, L. E.; Korgel, B. A.; Bard, A. J., *Science* **2002,** 296, (5571), 1293-1297.

43. Zhu, L.; Xu, L.; Tan, L.; Tan, H.; Yang, S.; Yao, S., *Talanta* **2012**.

44. Hong, L.; Liu, A.-L.; Li, G.-W.; Chen, W.; Lin, X.-H., *Biosensors and Bioelectronics* **2013,** 43, (0), 1-5.

45. VandeVord, P. J.; Matthew, H. W. T.; DeSilva, S. P.; Mayton, L.; Wu, B.; Wooley, P. H., *Journal of Biomedical Materials Research* **2002,** 59, (3), 585-590.

46. Mansouri, S.; Lavigne, P.; Corsi, K.; Benderdour, M.; Beaumont, E.; Fernandes, J. C., *European Journal of Pharmaceutics and Biopharmaceutics* **2004,** 57, (1), 1-8.

47. Woelfle, C.; Claus, R. O., *Nanotechnology* **2007,** 18, (2), 025402.

48. Dennany, L.; O'Reilly, E. J.; Innis, P. C.; Wallace, G. G.; Forster, R. J., *Electrochimica Acta* **2008,** 53, (13), 4599-4605.

49. Dennany, L.; Gerlach, M.; O'Carroll, S.; Keyes, T. E.; Forster, R. J.; Bertoncello, P., *Journal of Materials Chemistry* **2011,** 21, (36), 13984-13990.

50. Devadoss, A.; Dennany, L.; Dickinson, C.; Keyes, T. E.; Forster, R. J., *Electrochemistry Communications* **2012,** 19, 43-45.

51. Zou, G.; Ju, H., *Analytical Chemistry* **2004,** 76, (23), 6871-6876.

52. Jiang, H.; Ju, H., *Analytical Chemistry* **2007,** 79, (17), 6690-6696.

53. Rosenblum, L. T.; Kosaka, N.; Mitsunaga, M.; Choyke, P. L.; Kobayashi, H., *Contrast Media & Molecular Imaging* **2011,** 6, (3), 148-152.

AUTHOR INFORMATION

Corresponding Author

*WestCHEM. Department of Pure and Applied Chemistry, University of Strathclyde. 295 Cathedral Street, Glasgow, G1 1XL. Fax: +141 548 2535; Tel: +141 548 4322; Email: lynn.dennany@strath.ac.uk

ACKNOWLEDGMENT

This research is based upon works supported by the European Union 7th Framework programme, Marie Curie Reintegration Grant (PIRG-2010-268236).

LEGENDS

Figure 1. (a) Preparation of the modified GCE by drop-casting QD/chitosan composite, (b) preparation of the cholesterol/ChOx solution with incubation at 45°C for 60 minutes and (c) generation of QD ECL signal through interaction with H_2O_2 co-reactant, produced in the ChOx-catalysed oxidation of cholesterol.

Figure 2. The ECL spectrum of CdSeTe/ZnS QDs in 2mM H_2O_2 at a potential of -1.5 V *vs.* Ag/AgCl.

Figure 3. Current response for: (a) blank GCE in 0.1 M PBS (black line) and in 2 mM H_2O_2 (red line), (b) QD/chitosan film in 0.1 M PBS (black line), with 2 mM H_2O_2 (red line) and in 3 mM cholesterol (blue line) incubated with ChOx for 75 mins at 45°C. These were carried out at a scan rate of 100 mV s^{-1} over the potential range -2 V ≤**v**≤ -1 V *vs.* Ag/AgCl.

Figure 4. (a) ECL response of QD/chitosan film to increasing H_2O_2 concentration (0.25 (black line), 0.5 (red line), 1 (blue line), 2 (pink line), 3 (green line), 4 (navy line) and 5 (navy line) mM) at a scan rate of 100 mV s^{-1} over the potential range -1.6 ≤ **v**≤ -1.2 V *vs.* Ag/AgCl and (b) the linear dependence of ECL response with respect to [H_2O_2] for the QD/chitosan film. Error bars represent triplicate data points.

Figure 5. (a) ECL response of QD/chitosan film to increasing cholesterol concentration (0.25 (black line), 0.5 (red line), 0.75 (blue line), 1 (pink line), 1.5 (green line) and 2 (purple line) mM) at a scan rate of 100 mV s^{-1} over the potential range -1.6 ≤ **v**≤ -1.2 V *vs.* Ag/AgCl and (b) the linear dependence of ECL response with respect to [cholesterol] for the QD/chitosan film. Error bars represent triplicate data points.

Figure 6. The linear dependence of ECL response with respect to [cholesterol] for 3 independent biosensors.

Figure 7. Dependence of the ECL response at -1.35 V for the QD/chitosan film in 5 mM cholesterol with 10 mM urea, 10 mM glucose, 1 mg/mL citric acid and 10 mM uric acid. Error bars represent triplicate data points.

Figure 8. Dependence of the ECL response at -1.35 V with respect to [cholesterol] for the QD/chitosan film in spiked human serum samples. Red line indicates background signal intensity.

Figure 9. Dependence of the ECL response at -1.35 V with respect to [cholesterol] for the QD/chitosan/ChOx film. Error bars represent triplicate data points. Red line indicates background signal intensity.

Table1. Absorption and emission maxima of 2 μM Qdot 800 ITK QDs in PBS.

Table2. Average calculated concentrations and recoveries from unknown human serum samples.

FIGURE 1

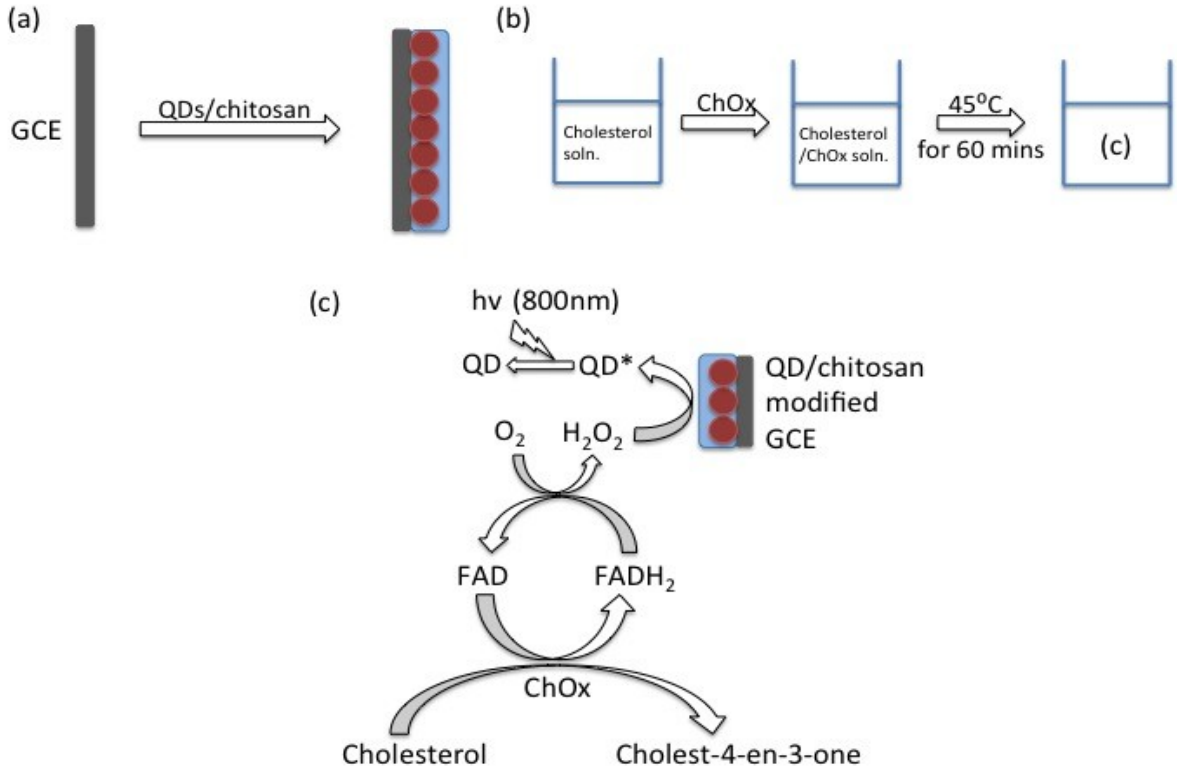
(a)
GCE
QDs/chitosan
(b)
Cholesterol soln.
ChOx
Cholesterol /ChOx soln.
45°C
for 60 mins
(c)
(c)
hv (800nm)
QD
QD*
QD/chitosan modified GCE
O2
H2O2
FAD
FADH2
ChOx
Cholesterol
Cholest-4-en-3-one

FIGURE 2

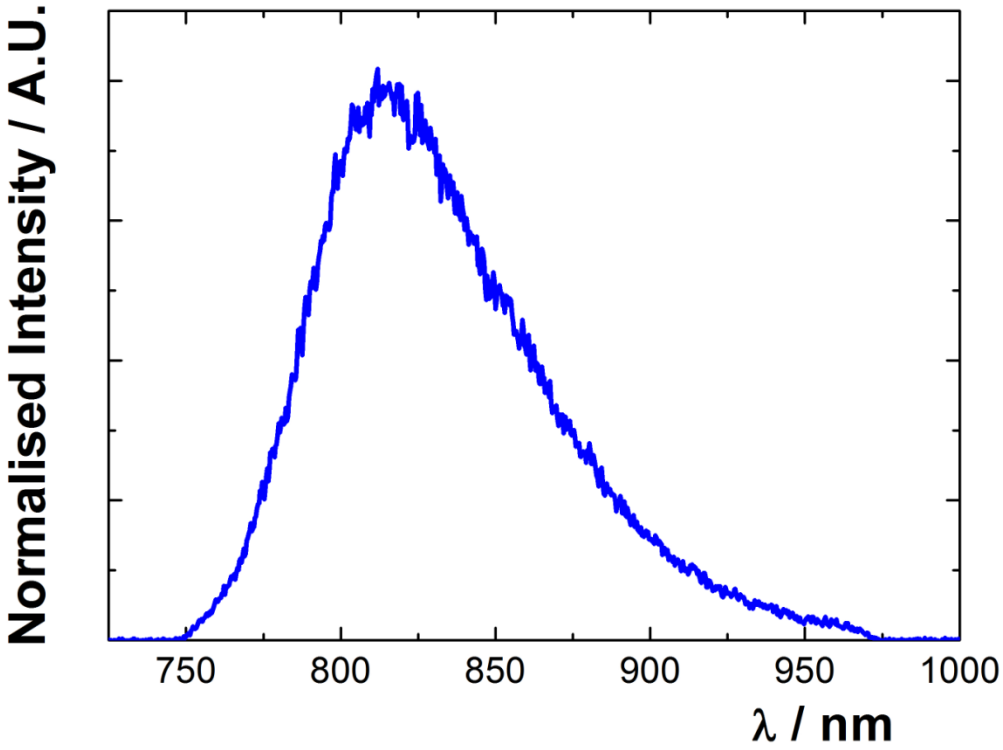

FIGURE 3

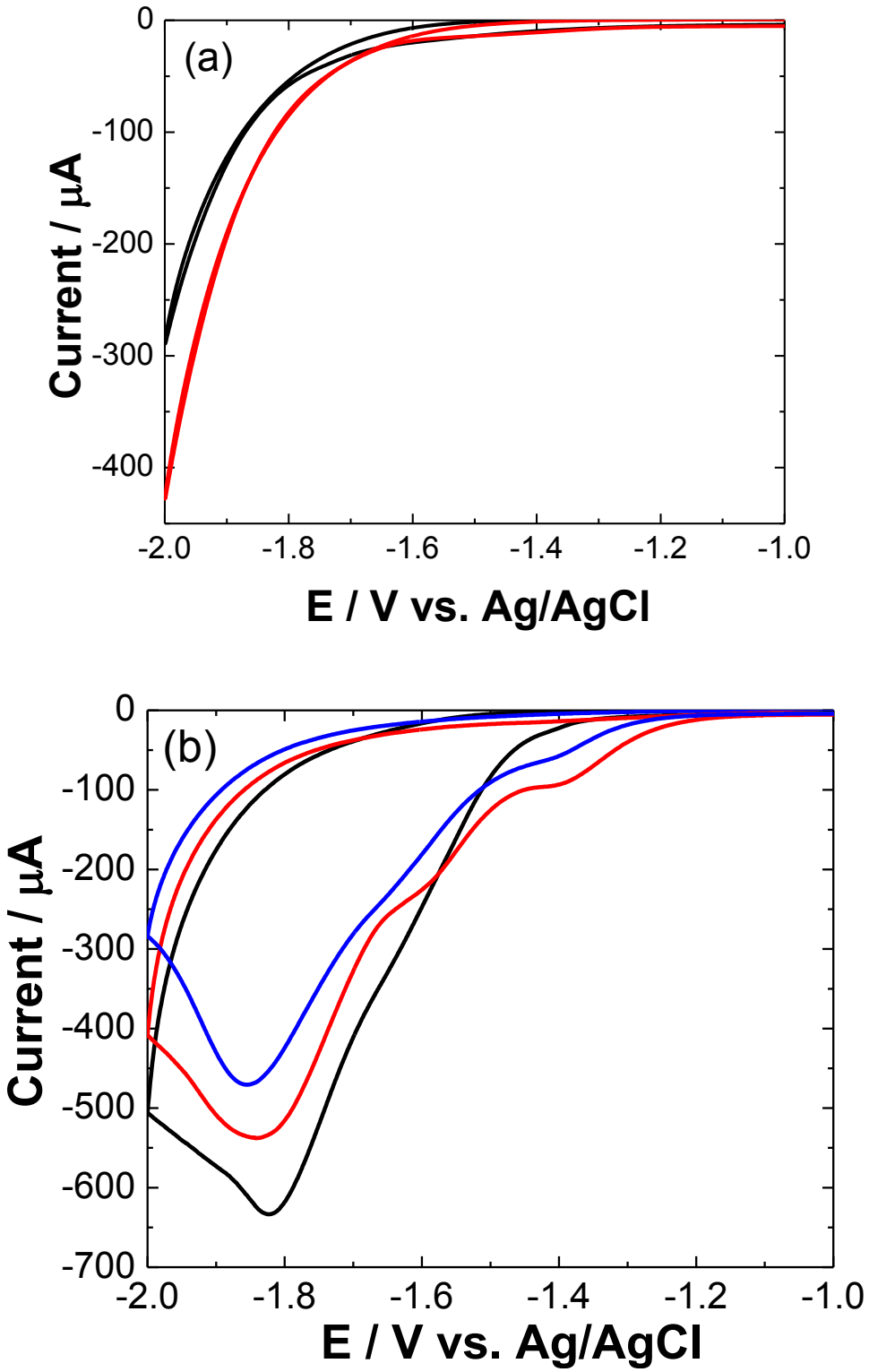
(a)
0
-100
-200
-300
-400
Current / µA
-2.0
-1.8
-1.6
-1.4
-1.2
-1.0
E / V vs. Ag/AgCl
(b)
0
-100
-200
-300
-400
-500
-600
-700
Current / µA
-2.0
-1.8
-1.6
-1.4
-1.2
-1.0
E / V vs. Ag/AgCl

FIGURE 4

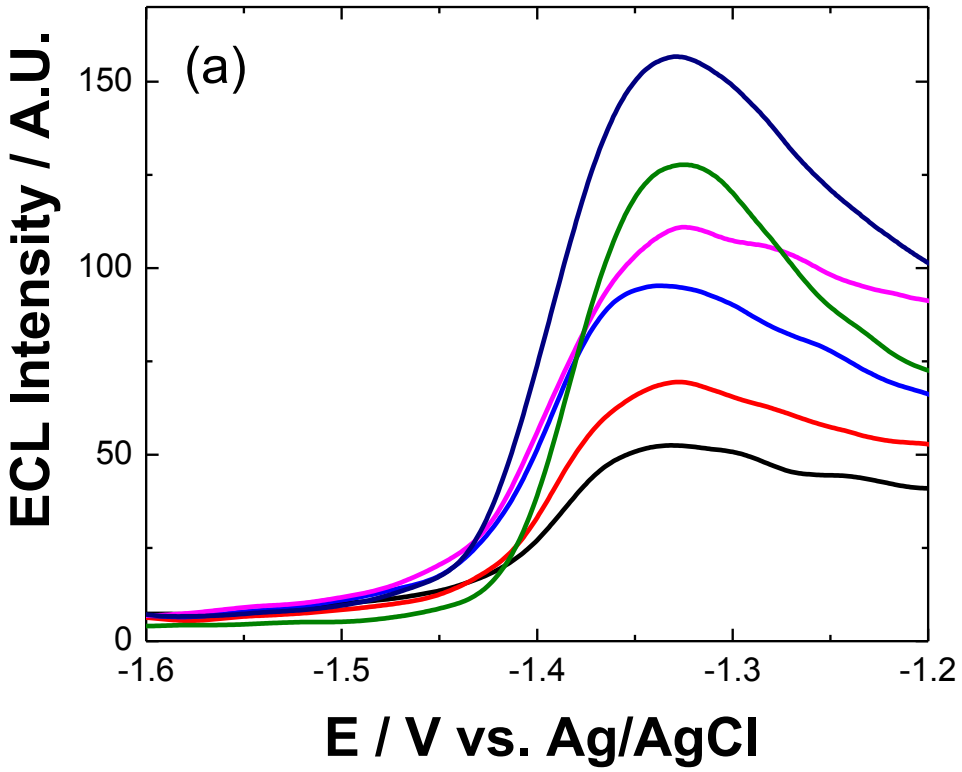
(a)
ECL Intensity / A.U.
150
100
50
0
-1.6
-1.5
-1.4
-1.3
-1.2
E / V vs. Ag/AgCl

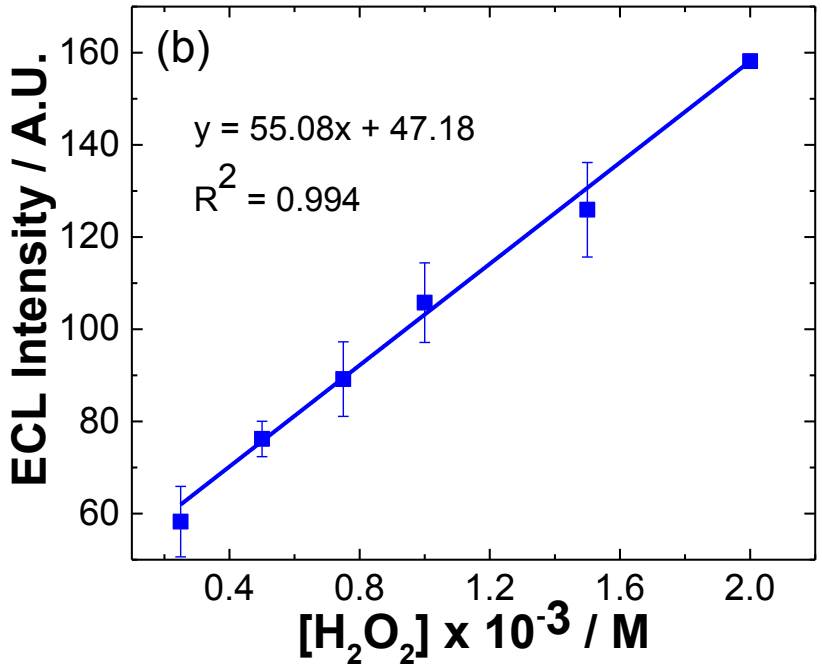
(b)
y = 55.08x + 47.18
R2 = 0.994
ECL Intensity / A.U.
160
140
120
100
80
60
0.4
0.8
1.2
1.6
2.0
[H2O2] x 10-3 / M

FIGURE 5

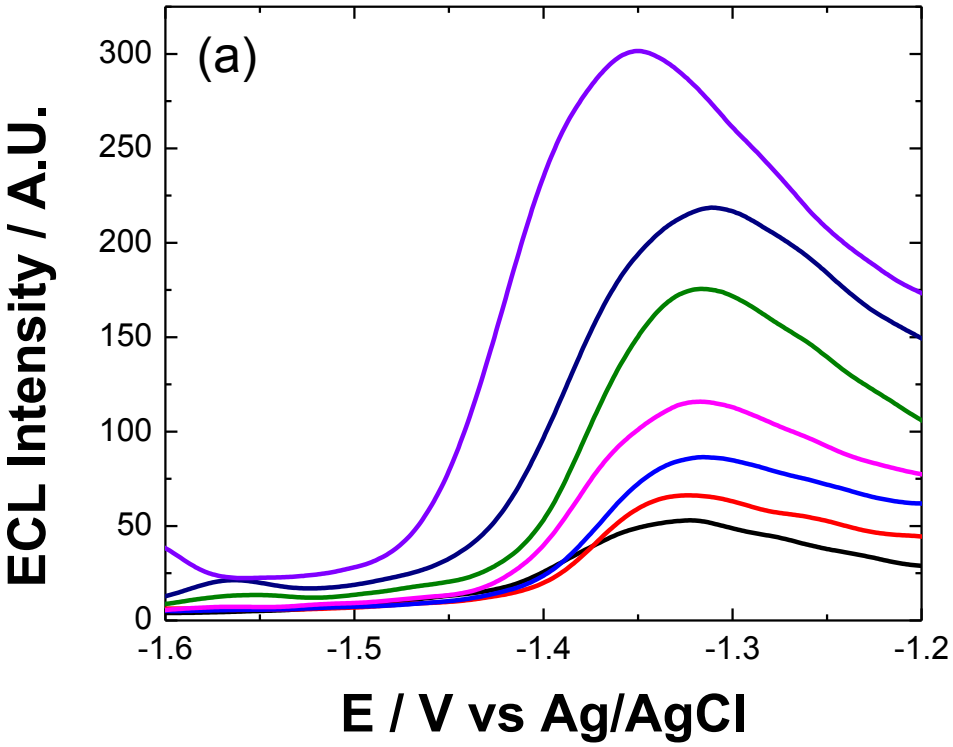
(a)
ECL Intensity / A.U.
300
250
200
150
100
50
0
-1.6
-1.5
-1.4
-1.3
-1.2
E / V vs Ag/AgCl

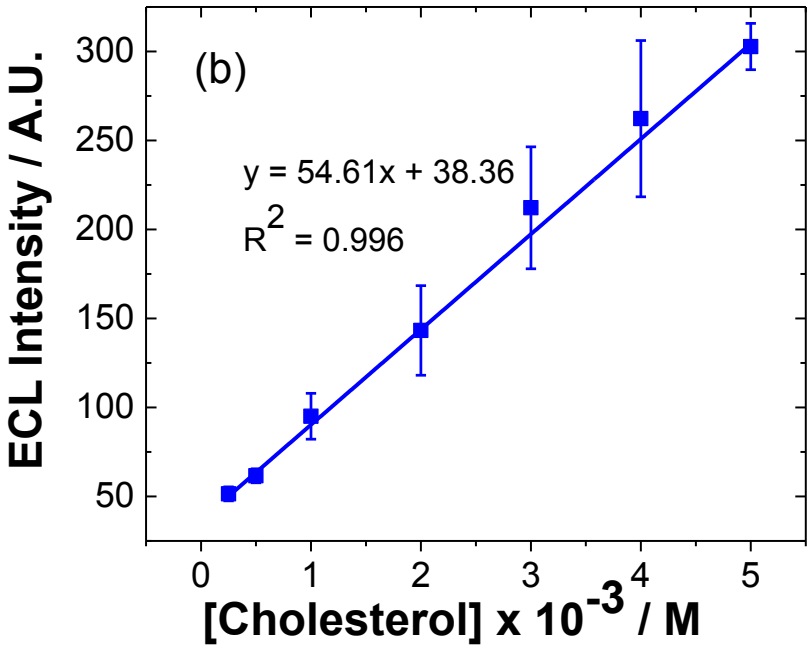
(b)
y = 54.61x + 38.36
R2 = 0.996
ECL Intensity / A.U.
300
250
200
150
100
50
0
1
2
3
4
5
[Cholesterol] x 10-3 / M

FIGURE 6

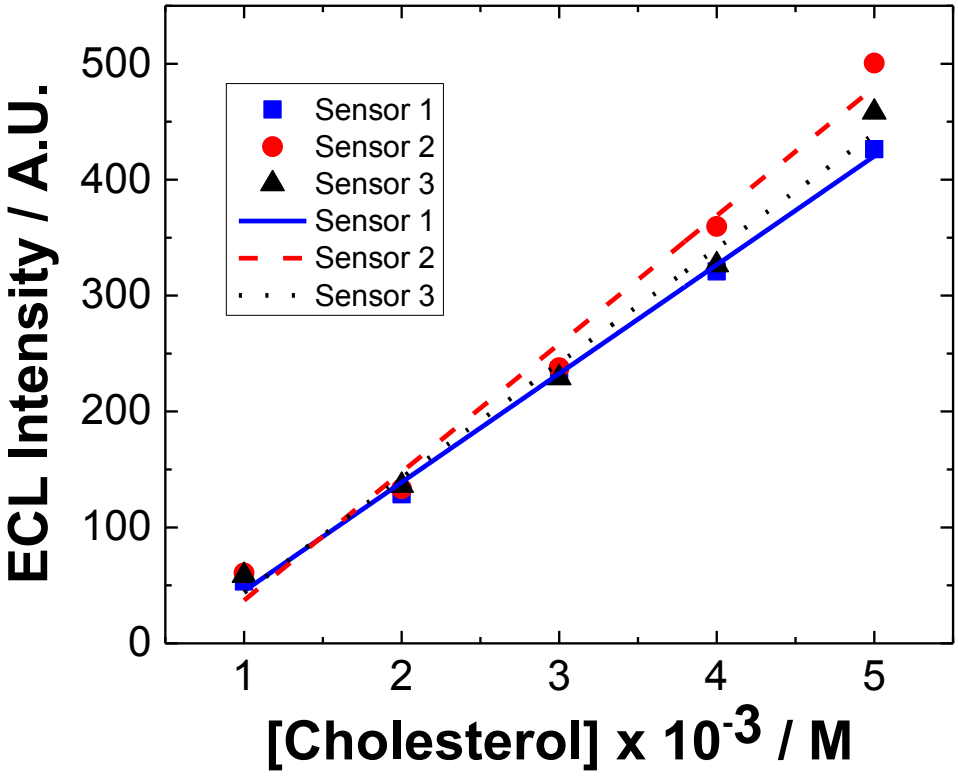
ECL Intensity / A.U.
0
100
200
300
400
500
1
2
3
4
5
[Cholesterol] x 10-3 / M
Sensor 1
Sensor 2
Sensor 3
Sensor 1
Sensor 2
Sensor 3

FIGURE 7

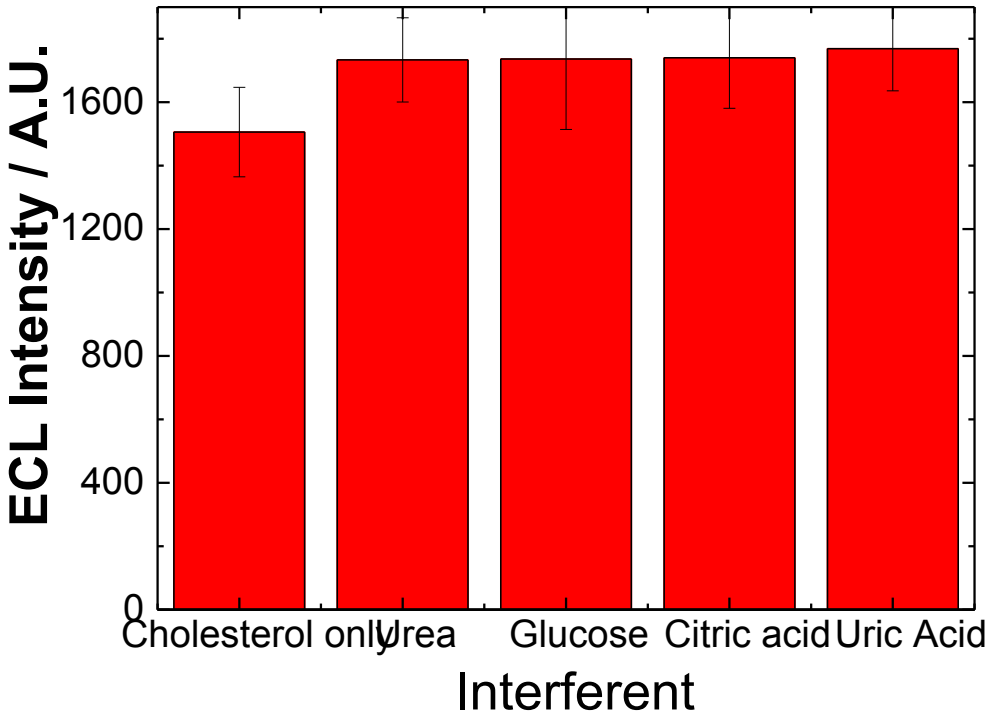
ECL Intensity / A.U.
0
400
800
1200
1600
Cholesterol only
Urea
Glucose
Citric acid
Uric Acid
Interferent

FIGURE 8

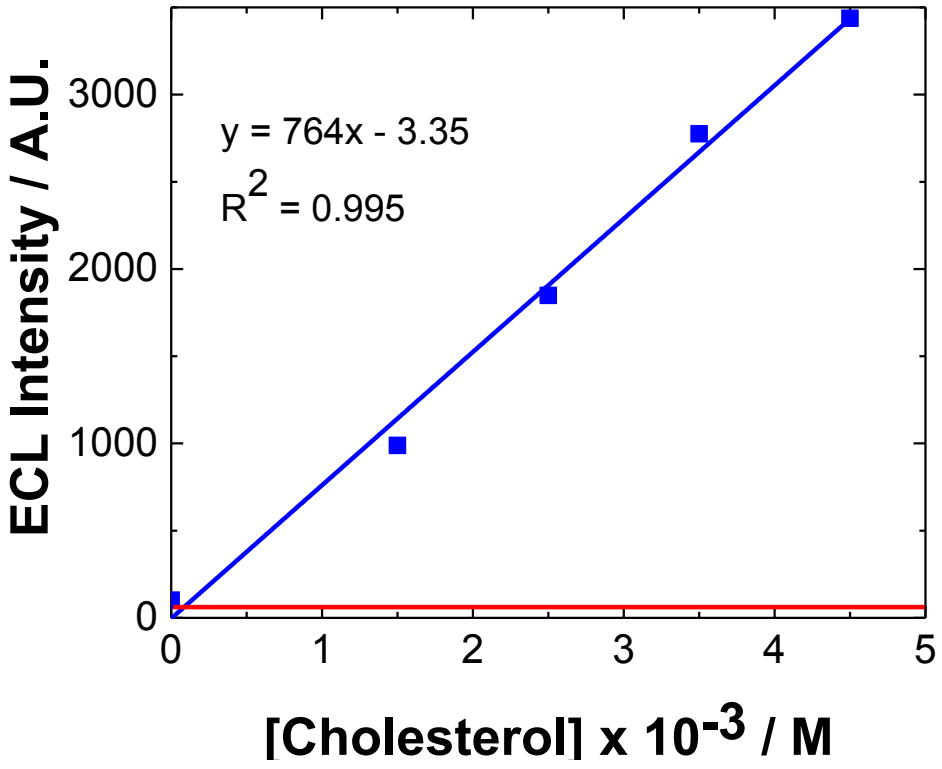
ECL Intensity / A.U.
3000
2000
1000
0
y = 764x - 3.35
R2 = 0.995
0
1
2
3
4
5
[Cholesterol] x 10-3 / M

FIGURE 9

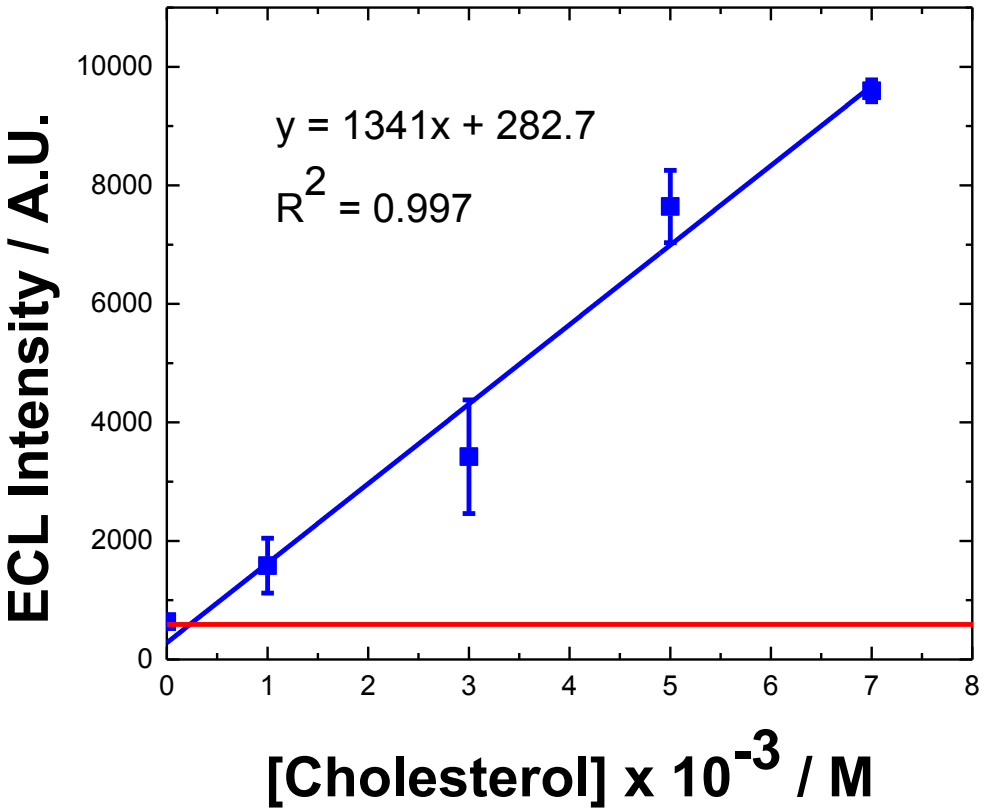
y = 1341x + 282.7
R2 = 0.997
ECL Intensity / A.U.
[Cholesterol] x 10-3 / M
0
2000
4000
6000
8000
10000
0
1
2
3
4
5
6
7
8

TABLE1

	Abs. maxima (nm)	Emission maxima (nm)
Qdot 800 ITK QDs	n/a[53]	795[53]

TABLE2

'Unknown' conc. (mM)	Average calc. conc. (mM)	% Recovery
2	1.86	93.10
3	3.24	107.85
4	3.63	90.82